

Dislocation Dynamics in Multiwalled Carbon Nanotubes at High Temperatures

J. Y. Huang,^{1,*} F. Ding,² and B. I. Yakobson^{2,*}

¹Center for Integrated Nanotechnologies (CINT), Sandia National Laboratories, Albuquerque, New Mexico 87185, USA

²Department of Mechanical Engineering and Materials Science, and the Department of Chemistry, Rice University, Houston, Texas 77005, USA

(Received 31 August 2007; published 23 January 2008)

Dislocation dynamics dictate the mechanical behavior of materials. Dislocations in periodic crystalline materials have been well documented. On the contrary, dislocations in *cylindrical* carbon nanotubes, particularly in multiwalled carbon nanotubes (MWCNTs), remain almost unexplored. Here we report that a room temperature $\frac{1}{2}\langle 0001 \rangle$ sessile dislocation in a MWCNT becomes highly mobile, as characterized by its glide, climb, and the glide-climb interactions, at temperatures of about 2000 °C. The dislocation glide leads to the cross-linking of different shells; dislocation climb creates nanocracks; and the interaction of two $\frac{1}{2}\langle 0001 \rangle$ dislocations creates kinks. We found that dislocation loops act as channels for mass transport. These dislocation dynamics are drastically different from that in conventional periodic crystalline materials due to the cylindrical, highly anisotropic structures of MWCNTs.

DOI: 10.1103/PhysRevLett.100.035503

PACS numbers: 61.72.Lk, 62.20.F-, 62.25.-g, 68.37.Lp

Dislocation dynamics dictate the mechanical behavior of materials [1]. Dislocations in periodic crystalline materials have been well documented [1]. On the contrary, dislocations in *cylindrical* carbon nanotubes, particularly in multiwalled carbon nanotubes (MWCNTs), remain almost unexplored due to their complicated structures [2–11]. There are fundamental differences, indeed. For example, the *Burgers' vector* \mathbf{b} —normally a topological invariant along any dislocation line—has its direction \mathbf{b} revolving along the loop in a cylindrical MWCNT. As a result, pure edge dislocation loop is possible, while it must change the type in a regular crystalline lattice, as any textbook explains. Another novelty or corollary is that *glide plane* becomes a spiral in the body of a nanotube. Besides the different topology, the atomistic structure is also affected by the lattice curvature (and partial sp^3 hybridization of the bonds).

Here we report the dynamical motion of a room temperature sessile $\frac{1}{2}\langle 0001 \rangle$ dislocation, as characterized by its glide, climb, and the glide and climb interactions, in a MWCNT at temperatures of about 2000 °C [8–10,12]. As a segment of the $\frac{1}{2}\langle 0001 \rangle$ edge dislocation loop bows out radially, it creates two screw dislocations bounding the two edge dislocations, cross-linking the different walls in a MWCNT. As the leading edge dislocation crosses more walls, the dislocation density increases, reminiscent of the dislocation multiplication in crystalline materials. Dislocation climb results in the formation of nanocracks, and the interaction between dislocation glide and climb creates kinks in the MWCNTs.

Our experiments were conducted inside a high-resolution transmission electron microscope (HRTEM) attached with a Nanofactory TEM-scanning tunneling microscopy (STM) platform [8–10,12]. Two terminal connections were made to individual MWCNTs by using the STM probe. We then passed a high current through the

MWCNT to heat it to a temperature ~ 2000 °C. At such high temperatures, dislocations that are generally sessile at room temperature are fully activated, and dislocation motion takes place.

Figure 1 shows the dynamics of dislocation glide, climb and glide-climb interactions in a MWCNT [13]. The dislocation with a Burgers vector of $\frac{1}{2}\langle 0001 \rangle$ is nucleated from the lower right wall [Fig. 1(a)] due to evaporation of carbon atoms or aggregation of vacancies, and then it migrates up along the edge of the same wall, leaving behind a nanocrack [Fig. 1(b)]. As the dislocation moves up to the middle of the MWCNT, it interacts with another dislocation formed due to the breakage of the innermost wall and with a Burgers vector of $\frac{1}{2}[000\bar{1}]$, forming a dislocation dipole [Fig. 1(c)], which then moves up together. As the dislocation dipole climbs up, the extra half plane on the right (the $\frac{1}{2}[0001]$ dislocation) becomes shorter and shorter due to loss of atoms; on the contrary, the one on the left (the $\frac{1}{2}[000\bar{1}]$ dislocation) grows along the edge. Apparently, atom exchanges have taken place, and it is very likely that atoms transport along the dislocation line from the right dislocation to the left one. In this context, a dislocation line provides a channel for mass transport. Note that the interaction of two edge dislocations also produces two screw dislocations, cross-linking the different walls. A detailed atomic structure of the dislocation [Fig. 1(c)] is shown in Figs. 1(e) and 1(f). It is seen that the two edge dislocations are connected by two screw dislocations, forming a dislocation loop, which links the different walls.

The two edge dislocations then annihilate each other, forming a kink in the nanotube walls [Fig. 1(d)]. The mechanism of how two dislocations interact to form a kink is illustrated in Figs. 1(g)–1(i). For ease of understanding, we use a two-dimensional graphite to illustrate how such interaction has taken place, and we anticipate that dislocation interaction in a MWCNT follows a similar

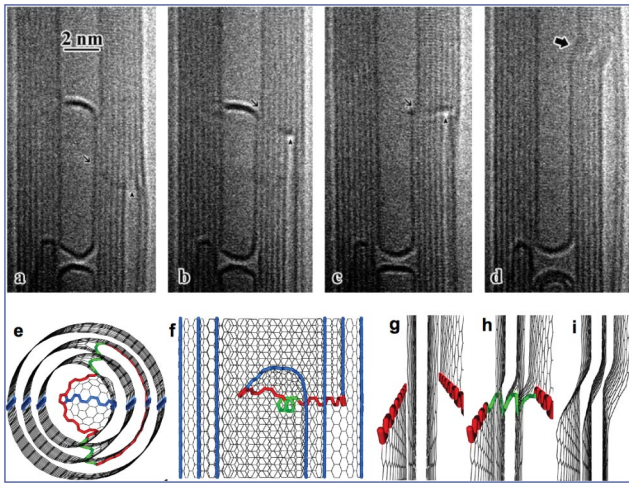


FIG. 1 (color). *In situ* dislocation dynamics in a MWCNT. Arrowheads and slim arrows point out the dislocation cores and the dislocation lines, respectively. The fat arrow points out a kink. The voltage applied to the nanotube was 2.55 V. The dislocation climb velocity is 19 nm/min. The core of the edge and screw dislocations in (e)–(i) is marked in red, and green, respectively: (a) A dislocation with a Burgers vector of $\frac{1}{2}[0001]$ is nucleated. (b) The dislocation climbs up. (c) A dislocation with a Burgers vector of $\frac{1}{2}[000\bar{1}]$ is formed, and it interacts with the climbing-up $\frac{1}{2}[0001]$ dislocation. (d) The $\frac{1}{2}[0001]$ dislocation annihilates with the $\frac{1}{2}[000\bar{1}]$ dislocation, forming a kink, (e)–(f) An atomic structural model of the dislocation in (c). The atoms marked in blue are for reference, (g)–(i) Schematic structural model explaining the kink formation due to the dislocation interaction.

route as that in a graphite. Figure 1(g) shows two edge dislocations with opposite signs of Burgers vectors. As part of the dislocation on the left glides towards the right, it pushes part of the 2nd layer (the leftmost layer is designated as the 1st layer, hereafter the same) to the 3rd layer, in the mean time, the glided out part of the 1st layer is now cross-linked to the 2nd layer via a screw dislocation, and the 2nd layer is cross-linked to the 3rd layer. . . Such a cross-linking essentially creates kinks in the bottom part of the graphite layers [Fig. 1(h)]. As more dislocations glide to the right, a complete kink forms [Fig. 1(i)], and both the screw and edge dislocations disappear. As the kink moves upward, it opens a crack behind it [Fig. 1(d)].

Figure 2 shows a dislocation motion in the same nanotube as shown in Fig. 1. The dislocation cores and the dislocation lines (marked by arrowheads and dashed lines) in the lower part of Fig. 2(a) are seen clearly. Interestingly, the dislocation line does not reside in the same wall, instead, its core is located between the 5th (the innermost wall is designated as the 1st wall, hereafter the same) and the 7th walls on the left, while between the 1st and 3rd walls on the right [Fig. 2(a)], indicating that the dislocation line crosses different walls. The dislocation then moves up, and interacts with another dislocation to form a closed dislocation loop [Fig. 2(b)]. The loop then moves upward [Fig. 2(c)], and the dislocation core remains at the same

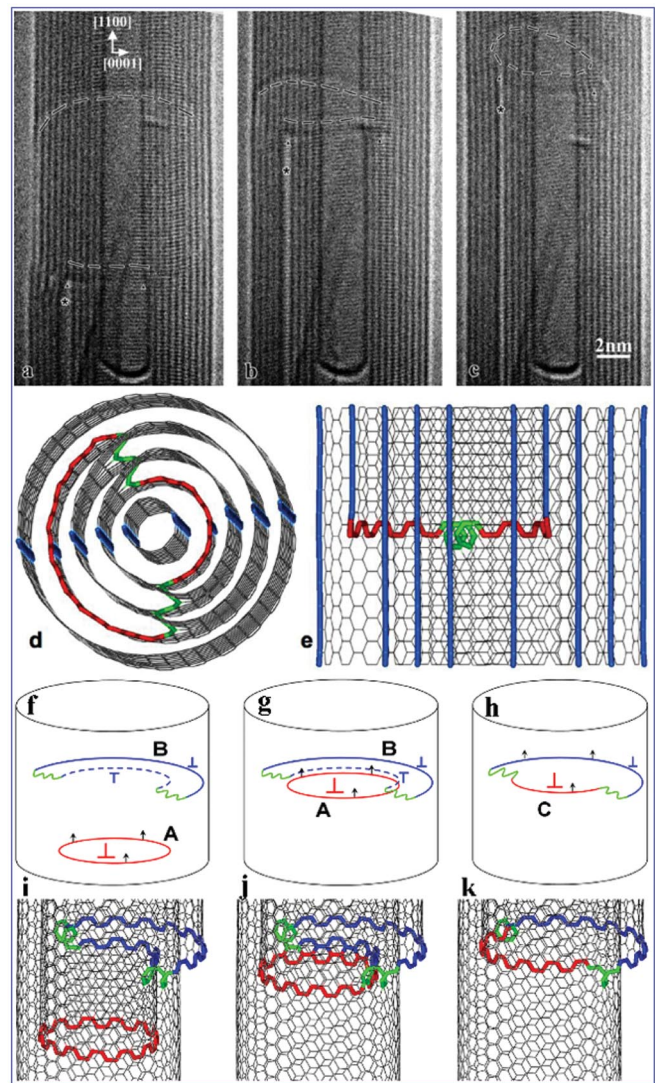


FIG. 2 (color). *In situ* dislocation dynamics in a MWCNT. The voltage applied to the nanotube was 2.55 V. The dislocation migration velocity is 8.5 nm/min. Arrowheads and dashed lines in (a)–(c) denote the dislocation cores and the dislocation lines, respectively. The stars mark nanocracks. The dislocation in the lower part of (a) climbs up, and it interacts with another dislocation (b), forming a dislocation loop (c). (d)–(e) An atomic structural model of the dislocation in (a). The atoms marked in blue are for reference. (f)–(k) Interactions of two dislocation loops, (f) the loop A is a pure edge dislocation loop (as shown by a symbol “ \perp ”) that encloses the tube hollow and tube axis. The loop B is a mixed loop located on one side of the tube hollow, and it does not enclose the tube hollow. The loop A climbs up to meet with the loop B (g). Part of the loop A and part of the loop B annihilate with each other forming a new dislocation loop C (h). The arrowheads in the figure show the climb direction of the dislocations, (i)–(k) Atomic structural models of the dislocation loops shown in (f)–(k), respectively.

wall on the left, while it crosses two walls and glides outward to between the 3rd and the 5th walls on the right. As the dislocation moves up, it creates a nanocrack behind it on the left wall, but not on the right wall. The climb

motion of the dislocation accompanied by the formation nanocracks are apparently attributed to the atom evaporation or vacancy generation at high temperatures and under electron beam irradiation.

The atomic structure of the dislocation in the lower part of Fig. 2(a) is shown in Figs. 2(d) and 2(e). It is seen that the dislocation forms a loop, which consists of two edge dislocations (red lines) and two screw dislocations (green lines). Again the dislocation loop links the different shells in the MWCNT. From the structural model [Figs. 2(d) and 2(e)], it is clear that the asymmetrical distribution of the dislocation lines in Figs. 2(a)–2(c) is attributed to the asymmetrical dislocation glide across the circumference of the nanotube.

We now turn our attention to the interactions of the two dislocation loops [Figs. 2(a)–2(c)]. There are two types of dislocation loops in a MWCNT: (i) the loop encloses the tube axis and its hollow [e.g., the loop in Fig. 3, and the loop A in Figs. 2(f)–2(k)]; (ii) the loop does not enclose

the tube axis or its hollow, but is located on one side of the outer rim of the tube hollow (e.g., the loop in Fig. 1, and the loop B in Figs. 2(f)–2(k)). The former dislocation loop cannot be shrunk to a point and disappear as in usual bulk material because of the topological double connectivity of the nanotube, where the dislocations cannot glide over the hollow core. In contrast, the latter type (ii) can shrink to a point and disappear, or form a kink [Figs. 1(c) and 1(d)]. When a dislocation loop of type (i) meets a dislocation loop of type (ii), part of both dislocation lines can annihilate and disappear. A new loop containing a part of loop (i) and part of loop (ii) is formed, as Figs. 2(f)–2(k) illustrate.

Figure 3 shows the dynamic motion of a closed dislocation loop from underneath the surface shell [Figs. 3(a) and 3(b)] to the surface [Fig. 3(c)] during the climbing-up process. Apparently dislocation glide has occurred. A schematic drawing of the dislocation glide mechanism is depicted in Figs. 3(d)–3(g). Assuming an edge dislocation in the inner wall [Fig. 3(d)], under stress [Fig. 3(e)] it glides outward. The stress could be due to the shrinkage of the lower-outer tube induced by atom sublimation or vacancy generation. Most likely only part of the dislocation glides out first, becoming the leading dislocation [red lines on the right of Fig. 3(f)], and the rest of the edge dislocation trails behind. The leading and trailing edge dislocations are bridged by two screw dislocations. Note that the lower segment of the outer wall is now connected to the edge dislocation (the joint blue and black lines in Fig. 3(f)). The dislocation loop moves around the circumference of the nanotube until the inner edge component completely glides out, and the dislocation thus moves one Burgers vector ($\frac{1}{2}[0001]$) outward [Fig. 3(g)]. It is interesting to note that the lower segment of the outer wall moves one Burgers vector inward, shrinking its diameter due to the dislocation migration [Fig. 3(g)]. Figure 3(h) is an atomic structural model of the dislocation shown in Fig. 3(f). The screw component is clearly seen from the top view [Fig. 3(i)], while the edge component is easily discernable from the side view [Fig. 3(j)].

It is now easy to understand the asymmetric distribution of the dislocation lines across the tube axis (Figs. 1 and 2). It is caused by the asymmetrical glide of dislocations [Figs. 1(e), 1(f), 2(d), 2(e), 3(f), 3(h), and 3(i)]. Consequently, the edge components of the dislocation can be located at different walls. Once the trailing dislocation sweeps around the entire circumference of the nanotubes, the original dislocation loop advances one Burgers vector outward radially ($\frac{1}{2}[0001]$). In the case of Fig. 3, the dislocation glides one Burgers vector outward to the surface.

The driving force for the dislocation dynamics observed here can be understood in terms of the inhomogeneous pressure build up induced by atom sublimation and vacancy/interstitial segregation, and the natural attraction of dislocations by free surfaces.

We suggest that the inhomogeneous pressure [14] inside the MWCNT plays a very important role in the dislocation

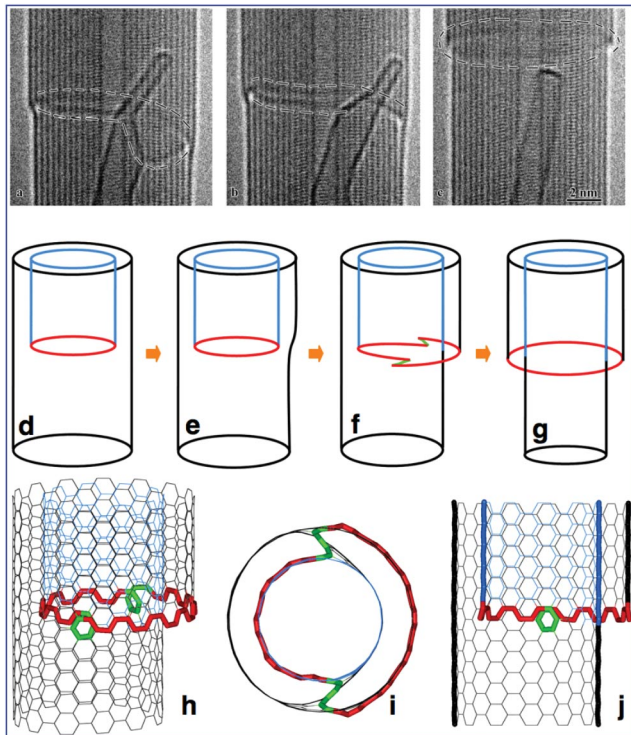


FIG. 3 (color). *In situ* dislocation dynamics in a MWCNT. The dashed lines in (a)–(c) denote the dislocation lines. The voltage applied to the nanotube was 2.55 V. The dislocation core is marked in red (edge components) and green (screw components) in (d)–(j). As the dislocation climbs up, it also glides from underneath the surface shell [(a),(b)] to the nanotube surface (c). The dislocation migration velocity is 1.8 nm/min. (d)–(g) Schematic drawing explaining the dislocation dynamics in (a)–(c). (d)–(e) An edge dislocation. (f) The edge dislocation slips out partly. (g) The dislocation slips completely out to the surface. (h)–(j) An atomic structural model of the dislocation in (f). The inner tube walls are shown in blue and the outer tube walls are shown in black.

dynamics. First, the temperature in the MWCNTs is estimated to be about 2000 °C [8–10,12] and at such high temperatures and under high-energy electron irradiation, each layer of the MWCNT tends to lose carbon atoms or dimers, and the emitted carbon atoms or dimers can be readsorbed. The outer layers are relatively easy to lose atoms since they are exposed to vacuum. And some of the knockout atoms are most likely to be deposited in the inner layers rather than on the outer layers. Thus inhomogeneous pressure may build up inside the MWCNTs as that in a carbon onion under irradiation at high temperatures [12,14–16].

The loss of carbon atoms [6,7] under our experimental conditions may also play a critical role in the dislocation dynamics in the MWCNTs. For example, as shown in Figs. 3(d)–3(g), the lower part of the outer wall becomes thinner as it connects to the upper part of the inner wall. Thus some carbon atoms must be removed by thermal sublimation or be knocked out by high-energy electrons, in our experimental conditions. The opposite process to that shown in Figs. 3(d)–3(g), i.e., dislocations gliding inward to the MWCNT, requires absorption of atoms. So it makes sense that dislocations glide outward in most of our experimental observations, which is because atoms are always lost from the MWCNTs due to sublimation and electron beam radiation under our experimental conditions.

Another important force that drives an edge dislocation outward is the natural attraction of a dislocation to a free surface, which is usually interpreted as interaction between such a dislocation and its image (antitwin, mirror image in the free surface plane) [1]. This force F is inversely proportional to the distance L between the dislocation and the surface, i.e., F (per unit length) $\sim G\mathbf{b}^2/(4\pi L)$, where G is the elastic shear modulus, \mathbf{b} is the Burgers vector. In a MWCNT, $G \sim 100$ GPa, $|\mathbf{b}| = 0.34$ nm, $L = 0.34$ nm, this yields $F \sim 2.7$ nN/nm. To bow out the loop shown in Fig. 3(c) purely by such an attraction force, F is about 80 nN.

The cross-linking of different walls in a MWCNT has important implications for the electrical, mechanical, and thermal properties of MWCNTs. For example, because of the cross-linking among the different walls, electrons and phonons are now able to transport through different walls simultaneously, in contrast to the nonlinked process, where transport of electrons between two different walls require hopping of electrons (at low bias) or thermal emission of electrons (at high bias), and transport of phonons are difficult if not impossible [11]. The cross-linking among the different walls may also prevent wall sliding during tensile loading experiments, thus improving the mechanical properties of MWCNTs.

We emphasize that the dislocation dynamics in a MWCNT can be rather complex due to the topological double connectivity, and it deserves further extensive systematic study. We believe that our models of the disloca-

tion dynamics reflect well our experimental observations, presenting the first attempt to describe these complicated structures.

This work was performed, in part, at the Center for Integrated Nanotechnologies, a U.S. Department of Energy, Office of Basic Energy Sciences user facility. Supported by Laboratory Directed Research and Development (LDRD), Sandia is a multiprogram laboratory operated by Sandia Corporation, a Lockheed Martin Company, for the United States Department of Energy's National Nuclear Security Administration under contract No. DE-AC04-94AL85000. J. Y. H. would like to thank Dr. Shuo Chen from MIT for making the STM tips, and Professor M. Vaziri at University of Michigan-Flint for providing the arc-discharged MWCNTs. Work at Rice University was supported by the National Science Foundation and by the Robert Welch Foundation.

*Corresponding authors.

jhuang@sandia.gov

biy@rice.edu

- [1] J. P. Hirth and J. Lothe, *Theory of Dislocations* (McGraw-Hill, New York, 1968).
- [2] A. Hashimoto, K. Suenaga, A. Gloter, K. Urita, and S. Iijima, *Nature (London)* **430**, 870 (2004).
- [3] A. Zobelli, C. P. Ewels, A. Gloter, G. Seifert, O. Stephan, S. Csillag, and C. Colliex, *Nano Lett.* **6**, 1955 (2006).
- [4] B. I. Yakobson, *Appl. Phys. Lett.* **72**, 918 (1998).
- [5] T. Dumitrica, M. Hua, and B. I. Yakobson, *Proc. Natl. Acad. Sci. U.S.A.* **103**, 6105 (2006).
- [6] F. Ding, K. Jiao, M. Q. Wu, and B. I. Yakobson, *Phys. Rev. Lett.* **98**, 075503 (2007).
- [7] F. Ding, K. Jiao, Y. Lin, and B. I. Yakobson, *Nano Lett.* **7**, 681 (2007).
- [8] J. Y. Huang, S. Chen, Z. Q. Wang, K. Kempa, Y. M. Wang, S. H. Jo, G. Chen, M. S. Dresselhaus, and Z. F. Ren, *Nature (London)* **439**, 281 (2006).
- [9] J. Y. Huang, S. Chen, Z. F. Ren, Z. Q. Wang, D. Z. Wang, M. Vaziri, G. Chen, and M. S. Dresselhaus, *Phys. Rev. Lett.* **97**, 075501 (2006).
- [10] J. Y. Huang, S. Chen, Z. F. Ren, Z. Wang, K. Kempa, M. J. Naughton, G. Chen, and M. S. Dresselhaus, *Phys. Rev. Lett.* **98**, 185501 (2007).
- [11] M. S. Dresselhaus, G. Dresselhaus, and Ph. Avouris, *Carbon Nanotubes: Synthesis, Structure, Properties, and Applications* (Springer, Heidelberg, 2001).
- [12] J. Y. Huang, *Nano Lett.* **7**, 2335 (2007).
- [13] See EPAPS Document No. E-PRLTAO-100-001801 for a supporting movie. For more information on EPAPS, see <http://www.aip.org/pubservs/epaps.html>.
- [14] L. Sun, F. Banhart, A. Krasheninnikov, J. A. Rodriguez-Manzo, M. Terrones, and P. M. Ajayan, *Science* **312**, 1199 (2006).
- [15] F. Banhart, *Rep. Prog. Phys.* **62**, 1181 (1999).
- [16] F. Banhart and P. M. Ajayan, *Nature (London)* **382**, 433 (1996).